

Observational constraints and geometrical diagnostics for generalized Chaplygin gas

Jianbo Lu*, Lixin Xu†, Baorong Chang and Yuanxing Gui

School of Physics & Optoelectronic Technology, Dalian University of Technology, Dalian, 116024, P. R. China

We apply the latest observational data: the Union supernovae (SNe), the observational Hubble data (OHD), the five-year WMAP and the SDSS baryon acoustic peak to constrain generalized chaplygin gas (GCG) model as the unification of dark matter and dark energy. It can be seen that the evolution of equation of state (EOS) of dark energy for GCG model is similar to the quiescence, and the cosmological constant model ($w_{de}(z) = -1$) is in 1σ confidence contour of the best fit dynamical $w_{de}(z)$. Furthermore, the best fit value of current equation of state $w_{0de} = -0.963 > -1$, and 1σ (68.3%) confidence level (CL) of w_{0de} is $-0.916 \geq w_{0de} \geq -1.010$ using above four data sets. At 2σ (95.4%) confidence level, it is shown that $-0.870 \geq w_{0de} \geq -1.057$. The best fit values of transition redshift and current deceleration parameter with confidence levels are $z_T = 0.741^{+0.048}_{-0.050}$ (1σ) $^{+0.096}_{-0.103}$ (2σ), $q_0 = -0.552^{+0.056}_{-0.055}$ (1σ) $^{+0.112}_{-0.111}$ (2σ). At last, we apply two geometrical diagnostics to GCG model to distinguish this scenario and Λ CDM. On the basis of cosmic observations we show the discriminations between these two models.

PACS numbers: 98.80.-k

1 Introduction

The type Ia supernovae (SNe Ia) investigations [1], the cosmic microwave background(CMB) results from WMAP [2] observations, and surveys of galaxies [3] all suggest that the expansion of present universe is speeding up rather than slowing down. Considering that the evolution of universe complies with the four-dimensional (4D) standard cosmology, the accelerated expansion of the present universe is usually attributed to the fact that dark energy (DE) is an exotic component with negative pressure. Many kinds of DE models have already been constructed such as Λ CDM [4], quintessence [5], phantom [6], quintom [7], generalized Chaplygin gas (GCG) [8], modified Chaplygin gas [9], holographic dark energy [10], agegraphic dark energy[11], and so forth. Furthermore, model-independent method [12][13][14][15][16][17] and modified gravity theories (such as scalar-tensor cosmology [18], Braneworld models [19]) to interpret accelerating universe have also been discussed.

On the one hand, on the basis of cosmic observations Akaike information criterion (AIC) and Bayesian information criterion (BIC) of model selection have been used to estimate which model for an accelerating universe is distinguished by statistical analysis [20]. It can be expected that model degeneration can be avoided by the accurate observational data in the future. On the other hand, one hopes that a general and model-independent manner can be used to distinguish DE models and show the discriminations between them. Refs. [21][22] introduced two geometrical methods, i.e., statefinder diagnostic and Om diagnostic. Statefinder parameters $\{r,s\}$ have been applied to a large number of DE models [21][23]. Recently, Om diagnostic is also presented in Ref. [22] to differentiate Λ CDM from other DE models and to understand the properties of DE. From Ref. [22], it can be seen that Ω_{0m} is a significant source of uncertainty for reconstructed equation of state (EOS) of DE w_{de} . However, for the constructed quantity Om , an important property is that it can be used to distinguish DE models in a robust manner with small influence from current matter density Ω_{0m} , i.e., even if uncertainties exist in the value of Ω_{0m} , Om evolution is not sensitive to its variation (current observations suggest an uncertainty of at least 25% in the value of Ω_{0m} [24]). In this paper, we apply Om and statefinder diagnostics to GCG model as the unification of dark matter and dark energy, and compare it with Λ CDM model. Furthermore, using the latest observational data: the Union SNe Ia [25], the observational Hubble data (OHD) [26], the five-year WMAP CMB shift parameter [27] and the baryon acoustic oscillation (BAO) peak from Sloan Digital Sky Survey (SDSS) [28] to GCG model, we get the values of transition redshift z_T , current deceleration parameter q_0 and equation of state of DE w_{0de} at 95.4% confidence level (CL).

The paper is organized as follows. In section 2, the GCG model as the unification of dark matter and dark energy is introduced briefly. Based on the recently observed data, the evolutions of cosmological quantities such as EOS of DE and deceleration parameter are given in section 3. In section 4, two geometrical diagnostic approaches are applied to GCG model. Section 5 is the conclusions.

2 generalized Chaplygin gas model

* lvjianbo819@163.com

† Corresponding author: lxxu@dlut.edu.cn

In the GCG approach, the most interesting property is that the unknown dark sections in universe–dark energy and dark matter, can be unified by using an exotic equation of state. The energy density ρ and pressure p are related by the equation of state [8]

$$p = -\frac{A}{\rho^\alpha}, \quad (1)$$

where A and α are parameters in the model.

Considering the Friedmann-Robertson-Walker (FRW) cosmology, by using the energy conservation equation: $d(\rho a^3) = -pd(a^3)$, the energy density of GCG can be derived as

$$\rho_{GCG} = \rho_{0GCG}[A_s + (1 - A_s)(1 + z)^{3(1+\alpha)}]^{\frac{1}{1+\alpha}}, \quad (2)$$

where a is the scale factor, $A_s = \frac{A}{\rho_0^{\frac{1}{1+\alpha}}}$. For the GCG model, as a scenario of the unification of dark matter and dark energy, the GCG fluid is decomposed into two components: the dark energy component and the dark matter component, i.e., $\rho_{GCG} = \rho_{de} + \rho_{dm}$, $p_{GCG} = p_{de}$. Then according to the relation between the density of dark matter and redshift:

$$\rho_{dm} = \rho_{0dm}(1 + z)^3, \quad (3)$$

the energy density of the DE in the GCG model can be given by

$$\rho_{de} = \rho_{GCG} - \rho_{dm} = \rho_{0GCG}[A_s + (1 - A_s)(1 + z)^{3(1+\alpha)}]^{\frac{1}{1+\alpha}} - \rho_{0dm}(1 + z)^3. \quad (4)$$

Next, we assume the universe is filled with two components, one is the GCG component, and the other is baryon matter component, i.e., $\rho_t = \rho_{GCG} + \rho_b$. The equation of state of dark energy can be derived as

$$w_{de} = \frac{p_{de}}{\rho_{de}} = \frac{-(1 - \Omega_{0b})A_s[A_s + (1 - A_s)(1 + z)^{3(1+\alpha)}]^{-\frac{\alpha}{1+\alpha}}}{(1 - \Omega_{0b})[A_s + (1 - A_s)(1 + z)^{3(1+\alpha)}]^{\frac{1}{1+\alpha}} - \Omega_{0dm}(1 + z)^3}, \quad (5)$$

where Ω_{0dm} and Ω_{0b} are present values of the dimensionless dark matter density and baryon matter component.

In a flat universe, making use of the Friedmann equation, the Hubble parameter H can be written as

$$H^2 = \frac{8\pi G\rho_t}{3} = H_0^2 E^2, \quad (6)$$

where $E^2 = (1 - \Omega_{0b})[A_s + (1 - A_s)(1 + z)^{3(1+\alpha)}]^{\frac{1}{1+\alpha}} + \Omega_{0b}(1 + z)^3$. H_0 denotes the present value of the Hubble parameter ("0" denotes the current value of the variable in this paper). When $\alpha = 1$, Eq. (6) is reduced to the CG scenario. Hence, the fractional energy densities of different components can be respectively expressed as

$$\Omega_{de} = \frac{(1 - \Omega_{0b})[A_s + (1 - A_s)(1 + z)^{3(1+\alpha)}]^{\frac{1}{1+\alpha}} - \Omega_{0dm}(1 + z)^3}{E^2}, \quad (7)$$

$$\Omega_{dm} = \frac{\Omega_{0dm}(1 + z)^3}{E^2}, \quad (8)$$

$$\Omega_b = \frac{\Omega_{0b}(1 + z)^3}{E^2}. \quad (9)$$

Furthermore, according the Eq. (6), deceleration parameter q can be obtained by

$$q = (1 + z)\frac{1}{H}\frac{dH}{dz} - 1. \quad (10)$$

In the following section, on the basis of Eq. (6), we will apply the recently observed data to GCG model to constrain the evolution of universe. For simplicity, we will displace model parameters (Ω_{0b}, A_s, α) with θ in the following section.

3 Constraint on EOS of dark energy and deceleration parameter

Since type Ia Supernovae behave as excellent standard candles, they can be used to directly measure the expansion rate of the universe up to high redshift for comparison with the present rate. Therefore, they provide direct information on the acceleration of the universe and constrain the DE model. Theoretical dark-energy model parameters are determined by minimizing the quantity

$$\chi_{SNe}^2(H_0, \theta) = \sum_{i=1}^N \frac{(\mu_{obs}(z_i) - \mu_{th}(H_0, \theta, z_i))^2}{\sigma_{obs;i}^2}, \quad (11)$$

where $N = 307$ for the Union SNe Ia data [25], which includes the SNe samples from the Supernova Legacy Survey (SNLS) [29], ESSENCE Surveys [30], distant SNe discovered by the Hubble Space Telescope (HST) [31], nearby SNe [32] and several other, small data sets. $\sigma_{obs;i}^2$ are errors due to flux uncertainties, intrinsic dispersion of SNe Ia absolute magnitude and peculiar velocity dispersion, respectively. θ denotes model parameters. The theoretical distance modulus μ_{th} is defined by

$$\mu_{th}(z_i) \equiv m_{th}(z_i) - M = 5 \log_{10}(D_L(z)) + 5 \log_{10}\left(\frac{H_0^{-1}}{Mpc}\right) + 25, \quad (12)$$

where

$$D_L(z) = H_0 d_L(z) = (1+z) \int_0^z \frac{H_0 dz'}{H(z'; \theta)}, \quad (13)$$

μ_{obs} is given by the supernovae dataset, and d_L is the luminosity distance.

The Hubble parameter $H(z)$ depends on the differential age of the universe as a function of redshift z in the form

$$H(z) = -\frac{1}{1+z} \frac{dz}{dt}. \quad (14)$$

Therefore, the value of $H(z)$ can directly be measured through a determination of dz/dt . By using the differential ages of passively evolving galaxies from the GDDS [33] and archival data [34], Simon *et al.* obtained nine values of $H(z)$ in the range of $0 < z < 1.8$ [26]. Using these nine observational Hubble data (OHD) we can constrain cosmological models by minimizing

$$\chi_{H_{ub}}^2(H_0, \theta) = \sum_{i=1}^N \frac{[H_{th}(z_i) - H_{obs}(H_0, \theta, z_i)]^2}{\sigma_{obs;i}^2}, \quad (15)$$

where H_{th} is the predicted value for the Hubble parameter, H_{obs} is the observed value, $\sigma_{obs;i}^2$ is the uncertainty of the measurement of standard deviation.

The structure of the anisotropies of the cosmic microwave background radiation depends on two eras in cosmology, i.e., the last scattering ear and today. They can also be applied to limit the model parameters of DE by using the shift parameter [35]

$$R = \sqrt{\Omega_{0m}^{eff}} \int_0^{z_{rec}} \frac{H_0 dz'}{H(z'; \theta)}, \quad (16)$$

where $z_{rec} = 1089$ is the redshift of recombination, and effective matter density parameter is given by $\Omega_{0m}^{eff} = \Omega_{0b} + (1 - \Omega_{0b})(1 - A_s)^{\frac{1}{1+\alpha}}$ [36][37][38]. R obtained from the five-year WMAP data is [27]

$$R = 1.715 \pm 0.021. \quad (17)$$

From the CMB constraint, the best fit values of parameters in the DE models can be determined by minimizing

$$\chi_{CMB}^2(\theta) = \frac{(R(\theta) - 1.715)^2}{0.021^2}. \quad (18)$$

Because the universe has a fraction of baryons, the acoustic oscillations in the relativistic plasma would be imprinted onto the late-time power spectrum of the non-relativistic matter [39]. Therefore, the acoustic signatures in the large-scale clustering of galaxies may also serve as a test to constrain models of DE with detection of a peak in the correlation function of luminous red galaxies in the SDSS [28]. By using the equation

$$A = \sqrt{\Omega_{0m}^{eff}} E(z_{BAO})^{-1/3} \left[\frac{1}{z_{BAO}} \int_0^z \frac{dz'}{E(z'; \theta)} \right]^{2/3}, \quad (19)$$

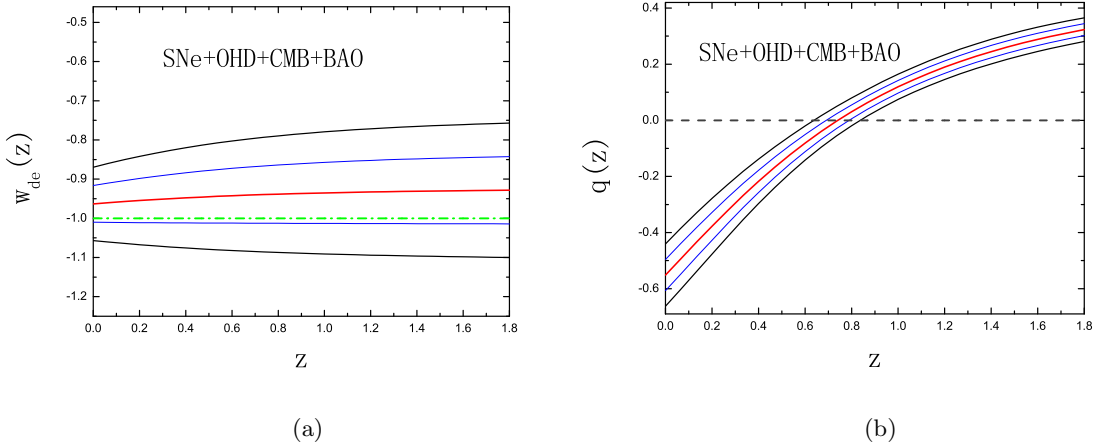


Fig. 1. The best fits of $w_{de}(z)$ and $q(z)$ with confidence level for GCG model. The red lines are drawn by using the best fit parameters. The blue lines show the 1σ CL, and the black lines show the 2σ CL. The green line shows the EOS of dark energy for Λ CDM model.

$A = 0.469 \pm 0.017$ as measured from the SDSS data, and $z_{BAO} = 0.35$, we can minimize the χ_{BAO}^2 defined by [40][41]

$$\chi_{BAO}^2(\theta) = \frac{(A(\theta) - 0.469)^2}{0.017^2}. \quad (20)$$

Here $E(z)$ is included in the Hubble parameter and can be given by defining $H(z) = H_0 E(z)$.

Next, using the datasets of the above observational techniques, we minimize the total likelihood χ_{total}^2

$$\chi_{total}^2 = \chi_{SNe}^2 + \chi_{Hub}^2 + \chi_{CMB}^2 + \chi_{BAO}^2. \quad (21)$$

Here H_0 contained in the $\chi_{total}^2(H_0, \theta)$ as a nuisance parameter is marginalized by integrating the likelihood $L(\theta) = \int dH_0 P(H_0) \exp(-\chi^2(H_0, \theta)/2)$. $P(H_0)$ is the prior distribution function of the present Hubble constant, and a Gaussian prior $H_0 = 100h \text{ km S}^{-1} \text{ Mpc}^{-1} = 72 \pm 8 \text{ km S}^{-1} \text{ Mpc}^{-1}$ [42] is adopted in the paper. Furthermore, one knows that the prior knowledge of cosmological parameter Ω_{ob} has been obtained by several other observations, such as $\Omega_{ob} h^2 = 0.0214 \pm 0.0020$ from the observation of the deuterium to hydrogen ratio towards QSO absorption systems [43], $\Omega_{ob} h^2 = 0.021 \pm 0.003$ from the BOOMERANG data [44] and $\Omega_{ob} h^2 = 0.022_{-0.003}^{+0.004}$ from the DASI results [45] for the observation of CMB. Then, in order to get the interesting result for the value of Ω_{ob} , we treat Ω_{ob} as a free parameter with Gaussian prior distribution centered in Ω_{ob}^{true} with spread $\sigma_{\Omega_{ob}-prior}$. And following Ref. [46], the "weak" prior for parameter Ω_{ob} will be used in our analysis, i.e., let it have a relative larger variable range $\Omega_{ob} h^2 = 0.0214 \pm 0.0060$ [46]. Thus, the $\chi_{total}^2(H_0, \theta)$ in Eq. (21) will be reconstructed as [47]

$$\chi_{total-prior}^2(\theta) = \chi_{total}^2(\theta) + \frac{(\Omega_{ob} - \Omega_{ob}^{true})^2}{\sigma_{\Omega_{ob}-prior}^2}, \quad (22)$$

where $\chi_{total}^2(\theta)$ denotes the total $\chi^2(\theta)$ obtained without imposing the prior knowledge of Ω_{ob} .

By using the maximum likelihood method for Eq. (22), we obtain the best fit values $(\Omega_{ob}, A_s, \alpha)$ in GCG model are $(0.0413, 0.734, -0.071)$ with $\chi_{min}^2 = 322.411$. It can be seen that the number of degrees of freedom (dof) is 313; here the value of dof of the model equals the number of observational data points minus the number of parameters. Then the reduced χ^2 value (i.e., the ratio of the χ_{min}^2 value and the number of dof) is given by $\chi_{min}^2/\text{dof} = 1.030$. According to Eqs. (5) and (10), the confidence level of the best fit $w_{de}(z)$ and $q(z)$ calculated by the covariance matrix are plotted in Fig. 1. From Fig. 1 (a), it is easy to see that the best fit value $w_{0de} \equiv w_{de}(z=0) = -0.963 > -1$, the 1σ (68.3%) confidence level of w_{0de} is $-0.916 \geq w_{0de} \geq -1.010$. Then the possibility of $w_{0de} < -1$ can't be excluded in 1σ level. Furthermore, it can be found that the best fit evolution of $w_{de}(z)$ for GCG is similar to the quiescence model ($w_{de}(z) = \text{const} \neq -1$), and the cosmological constant ($w_{de}(z) = -1$) is 1σ confidence contour of the best fit dynamical $w_{de}(z)$. At 2σ (95.4%) confidence level, it gives $-0.870 \geq w_{0de} \geq -1.057$.

One knows that the transition redshift z_T denotes the time when the evolution of the universe changes from decelerated expansion to accelerated expansion. The larger value of z_T we have, the earlier is the time of turning into an accelerating universe. The value of q_0 indicates the expansion rhythm of the present universe. The smaller

value of q_0 we have, the more violent is the acceleration of the universe. From Fig. 1 (b), we can see that the best fit values of transition redshift and current deceleration parameter with confidence levels are $z_T = 0.741^{+0.048}_{-0.050}$ (1σ) $^{+0.096}_{-0.103}$ (2σ), $q_0 = -0.552^{+0.056}_{-0.055}$ (1σ) $^{+0.112}_{-0.111}$ (2σ). It can be seen that, at 1σ confidence level, the value of z_T from our constant is larger than the result in Ref. [48], and the cosmic constraints on z_T (2σ) and q_0 (1σ) are more stringent than the results in Ref. [48], where $z_T = 0.49^{+0.14}_{-0.07}$ (1σ) $^{+0.54}_{-0.12}$ (2σ) and $q_0 = -0.73^{+0.21}_{-0.20}$ (1σ), are obtained from Union SNe Ia data by using a linear two-parameter expansion for the decelerating parameter, $q(z) = q_0 + q_1 z$.

4 Determining Om and statefinder diagnostic for GCG model from cosmic observations

4.1 Om diagnostic for GCG model

In order to interpret accelerating universe, many kinds of dark energy models have been constructed. They are introduced from different theories or methods, so a general and model-independent manner to distinguish these models are necessary. In what follows, we apply two geometrical approaches, i.e., Om diagnostic and statefinder diagnostic, to the GCG model as the unification of dark energy and dark matter. And we compare the results with Λ CDM model to find the differences between these two models.

It is well known that model-independent quantity $H(z)$ is important to understand the properties of DE, since its value can be directly obtained from cosmic observations (for example, the relation between luminosity distance D_L and Hubble parameter is $H(z) = [\frac{d}{dz}(\frac{D_L(z)}{1+z})]^{-1}$ [22][49][50] for SNe investigations). Recently, a new diagnostic of dark energy Om is introduced to distinguish DE models. The starting point for Om diagnostic is the Hubble parameter and it is defined as [22]

$$Om(x) \equiv \frac{E^2(x) - 1}{x^3 - 1}, \quad E(x) = H(x)/H_0, \quad x = 1 + z. \quad (23)$$

It can be regarded as a robust indicator of DE. For Λ CDM model, $Om(z) = \Omega_{0m}$ is a constant. For dark energy with a constant EOS of DE, $w_{de}(z)=\text{const}$, a negative slope of $Om(z)$ is suggestive of quintessence ($w_{de}(z) > -1$) while a positive slope of $Om(z)$ indicates phantom ($w_{de}(z) < -1$) [22].

Furthermore, from Ref. [22], one can see that the evolution of reconstructed EOS of DE $w_{de}(z)$ is very sensitive to the given value of matter density Ω_{0m} . The larger error for reconstructed $w_{de}(z)$ can be produced by the erroneous estimation of Ω_{0m} . However, since the matter density Ω_{0m} is not explicitly entered into the definition of $Om(z)$ (23), for the reconstructed $Om(z)$, the influence of Ω_{0m} on $Om(z)$ is relative smaller. Thus, for the reconstructed scenario $Om(z)$ is a better quantity than $w_{de}(z)$ to truly distinguish DE models and to show the properties of DE.

From Eq. (6), we can see that the expression of $H(z)$ for GCG model as a unified dark sector only includes baryon matter density Ω_{0b} and other two model parameters (A_s, α), unlike other DE models such as Λ CDM [4], quintessence [5], phantom [6], quintom [7], model-independent methods [13][14][15][16], etc. [51], where Hubble parameter explicitly include the parameter Ω_{0m} . Furthermore, one knows that the value of Ω_{0b} and its uncertainty from observational constraints are smaller relative to Ω_{0m} . Then the influence of uncertainty of Ω_{0b} on $Om(z)$ should be smaller comparing with Ω_{0m} . We use a combination of the Union SNe Ia data and the nine observational Hubble data to plot the evolutions of $Om(z)$ for GCG model with different values of Ω_{0b} in Fig. 2 (upper). It can be seen that at a larger variable range for Ω_{0b} , evolution of $Om(z)$ is almost independent of its variation. Here we do not use the reconstructed scenario as did in Ref. [22]. On the other hand, for $w_{de}(z)$ it can be seen that both Ω_{0b} and Ω_{0dm} are included in its expression for GCG model (5). And the evolutions of $w_{de}(z)$ for GCG model with different values of $\Omega_{0m}(= \Omega_{0b} + \Omega_{0dm})$ are also plotted from the Union SNe Ia data and the nine observational Hubble data in Fig. 2 (lower). It is shown that the evolution of $w_{de}(z)$ is quite sensitive to the given value of matter density Ω_{0m} , which is consistent with the conclusion of reconstructed scenario for w_{de} in Ref. [22].

In Ref. [52], Om diagnostic has been used to distinguish Λ CDM and Ricci DE model. Assuming the matter density Ω_{0m} to be a free parameter, Ref. [22] plots the evolution diagram of $Om(z)$ from three cosmic observations: the Union SNe Ia data, the five year WMAP and the SDSS baryon acoustic peak, by using a model-independent CPL ansatz (it is an expansion for EOS of DE relative to scale factor a , $w_{de}(a) = w_0 + w_1(1 - a)$, or $w_{de}(z) = w_0 + \frac{w_1 z}{1+z}$ [16][53]). In this paper, treating Ω_{0b} as a free parameter, we use the Om diagnostic to GCG model. From above, it is shown that at an interesting range for the value of Ω_{0b} , the evolution of $Om(z)$ for GCG model is almost independent of baryon matter density Ω_{0b} , while the evolution of $w_{de}(z)$ is very sensitive to the variation of Ω_{0m} . These results are consistent with Ref. [22], where authors use the reconstructed scenario for cosmological quantities $Om(z)$ and $w_{de}(z)$. Then for GCG model as the unification of dark matter and dark energy, we do not reconstruct $Om(z)$ by using parametric [50][54] or non-parametric [55] methods as shown in Ref. [22]. Furthermore, one knows when the same cosmic observational datasets are used, different dark energy models give different predictions of cosmological history. On the other hand, cosmic constraints on the same dark energy model are also dependent on observational

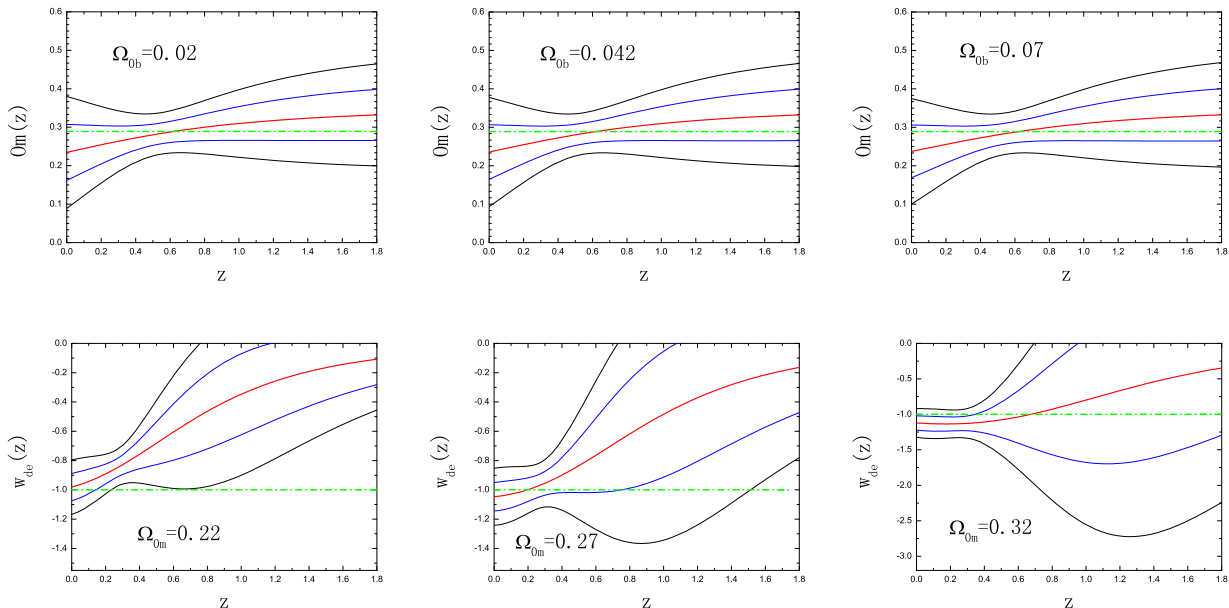


Fig. 2. Evolutions of $Om(z)$ and $w_{de}(z)$ from a combination of Union SNe and OHD data using the GCG model. Here three different values $\Omega_{0b}=0.02, 0.042, 0.07$ for $Om(z)$ evolution diagram, and $\Omega_{0m} = \Omega_{0b} + \Omega_{0dm}=0.22, 0.27, 0.32$ (i.e., $\Omega_{0dm}=0.2, 0.228, 0.25$) for w_{de} diagram are assumed. The red lines show the best fit evolutions of $Om(z)$ and $w_{de}(z)$ from cosmic observations. The blue lines show the 1σ CL, and the black lines show the 2σ CL. The green lines show the values of $Om(z)$ and $w_{de}(z)$ for Λ CDM model.

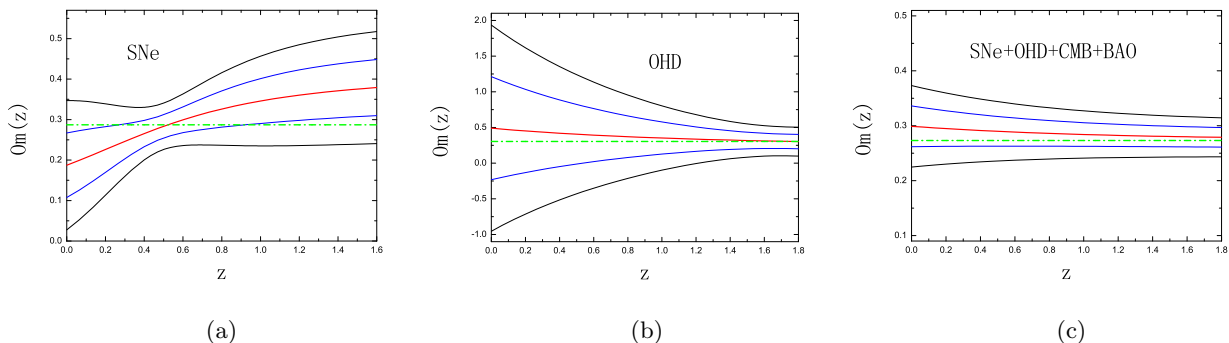


Fig. 3. $Om(z)$ diagnostic for GCG model from cosmic observations: Union SNe data, OHD data, and a combination of Union SNe, OHD, CMB and BAO data. Here Ω_{0b} is treated as a free parameter. The red lines show the best fit evolutions from cosmic observations. The blue lines show the 1σ CL, and the black lines show the 2σ CL. The green lines show the values of $Om(z)$ for Λ CDM model obtained from the corresponding cosmic constraint.

data, i.e., different evolutions of cosmological quantity can be obtained from different datasets even if the same model is used. This is the so-called data-dependent. As an example, here we use the Union SNe Ia data and the OHD data to plot the evolution of $Om(z)$ in Fig. 3 (a) and (b), respectively. And in order to diminish systematic uncertainties and get the stringent constraints on cosmological quantity, we also combine four cosmic observations: the Union SNe Ia data, the OHD data, the five year WMAP, and the SDSS baryon acoustic peak to constrain the evolution of $Om(z)$ for GCG model (see Fig. 3 (c)).

From Fig. 3, we can see the differences between GCG and Λ CDM model according to the best fit evolutions of $Om(z)$. And it is shown that $Om(z)$ diagram for GCG model is different when different observational data is used. For the constraint from the Union SNe Ia data, the difference between GCG and Λ CDM is obvious, while for the cases of the combined constraint and the OHD constraint, the best fit evolutions of $Om(z)$ for GCG model are near to Λ CDM case. Next we consider the case of combined constraint. From Fig. 3 (c), it can be seen that $Om(z=0) = 0.299^{+0.037}_{-0.037}$ (1σ) $^{+0.074}_{-0.074}$ (2σ) for GCG model. Furthermore, using above four observed data to Λ CDM

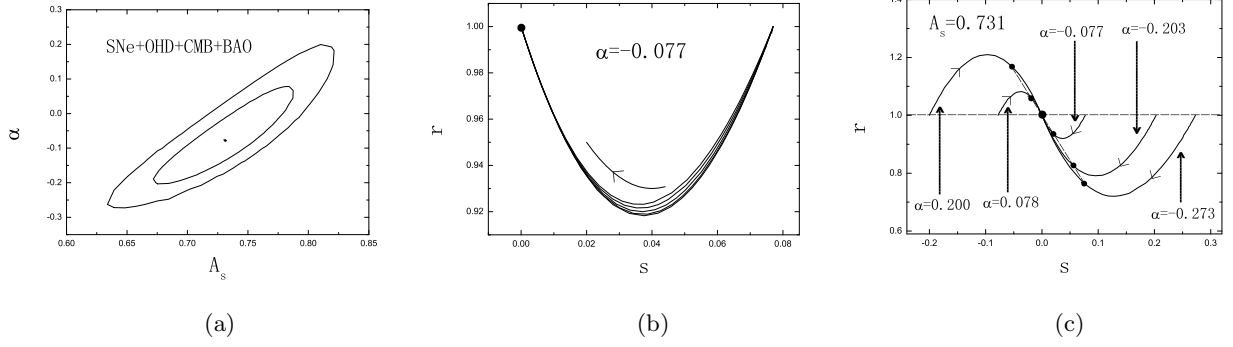


Fig. 4. The 68.3% and 95.4% confidence level contours for GCG model parameter A_s versus α (a), and statefinder diagnostic for GCG model (b), (c). Here according to the combined constraint, the best fit value $\alpha = -0.077$ is given, and A_s is setted as (0.634, 0.672, 0.731, 0.784, 0.821), respectively in (b); the best fit value $A_s = 0.731$ is given, and α is setted as (-0.273, -0.203, -0.077, 0.078, 0.200), respectively in (c). Furthermore, in Figures (b) and (c) the bigger dots locate the Λ CDM fixed point (1,0), the smaller dots locate the current values of the statefinder pair $\{r, s\}$, and arrows denote the evolution directions of the statefinder trajectories $r(s)$.

model, we get the best fit value of Ω_{0m} and its confidence levels, $\Omega_{0m} = 0.273^{+0.016}_{-0.015}$ (1σ) $^{+0.033}_{-0.030}$ (2σ). We know $Om(z) = \Omega_{0m}$ for Λ CDM, then the best fit evolution of $Om(z)$ for Λ CDM model is in the 1σ confidence level of $Om(z)$ evolution for GCG model. And we can see that at 1σ and 2σ confidence level, these two models can not be clearly distinguished by current observed data according to their $Om(z)$ evolutions. In other words, current cosmic observations can not exclude either one for these two models according to the $Om(z)$ diagrams. Here it should be noted that, the Hubble parameter for GCG model as the unification of dark matter and dark energy only depends on baryon density Ω_{0b} explicitly for the parameters of denoting matter density component, but does not explicitly include the cosmological quantity Ω_{0m} . And this method for differentiating these two models is almost independent of the quantity Ω_{0b} .

4.2 Constraint on GCG model parameter and statefinder diagnostic

According to document [21], another diagnostic of dark energy called statefinder is defined as follows:

$$r \equiv \frac{\ddot{a}}{aH^3}, \quad s \equiv \frac{r-1}{3(q-\frac{1}{2})}. \quad (24)$$

Next, we apply statefinder parameters $\{r, s\}$ to GCG model. Like the $Om(z)$ (23), statefinder only depends upon the scale factor a and its derivative. So, both of them are "geometrical" diagnostics. It can be seen that the statefinder parameters $\{r, s\}$ involve the third derivative of the scale factor $a(t)$, while Om depends upon its first derivative only. Trajectories in the $r-s$ plane corresponding to different cosmological models exhibit qualitatively different behaviors. And for Λ CDM model, $\{r, s\} = \{1, 0\}$ is a fixed point [21].

Furthermore, we can also derive the concrete expressions of the statefinder parameters

$$r = 1 + \frac{9}{2}w_{de}\Omega_{de}(1+w_{de}) - \frac{3}{2}\Omega_{de}\frac{\dot{w}_{de}}{H}, \quad s = 1 + w_{de} - \frac{\dot{w}_{de}}{3w_{de}H}. \quad (25)$$

Here w_{de} and Ω_{de} are given by Eqs. (5) and (7) for GCG model, respectively.

By using the latest observational data: the Union SNe Ia, the observational Hubble data, the five-year WMAP and the SDSS baryon acoustic peak to GCG model, the 68.3% and 95.4% confidence level contours for model parameters (A_s, α) are plotted in Fig. 4 (a). From Fig. (4) (a), we can see that the best fit values of model parameters and their confidence levels are $A_s = 0.731^{+0.053}_{-0.059}$ (1σ) $^{+0.090}_{-0.097}$ (2σ), $\alpha = -0.077^{+0.155}_{-0.126}$ (1σ) $^{+0.277}_{-0.196}$ (2σ). It can be seen that this constraint on parameter α is more stringent than the results from Refs. [37][38], where the results of constraint on GCG model parameters are $A_s = 0.70^{+0.16}_{-0.17}$ and $\alpha = -0.09^{+0.54}_{-0.33}$ at 2σ confidence level by using the X-ray gas mass fractions of galaxy clusters, the dimensionless coordinate distance of SNe Ia and FRIB radio galaxies [37], and $A_s = 0.75^{+0.08}_{-0.08}$, $\alpha = 0.05^{+0.37}_{-0.26}$ at 2σ confidence level from the nine observational Hubble data, the 115 SNLS SNe Ia data and the SDSS baryonic acoustic oscillations peak [38].

Next according to the constraint results of model parameter (A_s, α) in Fig. 4 (a), we use the statefinder parameters to discriminate the GCG and Λ CDM model. From $r-s$ planes (Fig. 4 (b) and (c)), it can be found that the difference

for these two model is obvious. For Fig. 4 (b), according to the combined constraint, the best fit value $\alpha = -0.077$ is fixed and A_s is setted by the best fit value and critical values at 1σ and 2σ confidence level (0.634, 0.672, 0.731, 0.784, 0.821), respectively. From Fig. 4 (b), it can be seen that $r(s)$ evolution diagram is not sensitive to the variation of value of model parameter A_s . For Fig. 4 (c), the best fit value $A_s = 0.731$ is fixed, and α is setted as (-0.273, -0.203 -0.077, 0.078, 0.200) from constraint result, respectively. And it is obvious that the shape of $r(s)$ diagram for this case much depends on the value of model parameter α . Especially, since it can be calculated that when $\alpha = 0$, one gets $r = 1$, $s = 0$ (here virtual number is setted as sixteen). Thus, for Fig. 4 (c) it can be divided to two regions according to the value of parameter α : when $\alpha > 0$, one gets $r > 1$, $s < 0$; when $\alpha < 0$, one gets $r < 1$, $s > 0$. However, when z tends to -1, no matter what value of α is, we have $\{r, s\} \simeq \{1, 0\}$, i.e., GCG model tends to Λ CDM model in the distant future. Furthermore, we can see that the larger value of α we have, the larger peak value is for r . And from Fig. 4 (c), it is shown that the present statefinder points, $\{r_0, s_0\}$, locate on a straight line. This is because when $z = 0$, the relationship between r_0 and s_0 is linear, $r_0 = 1 + w_{0de}\Omega_{0de}s_0$, and w_{0de} , Ω_{0de} are constant at this time.

5 Conclusion

In summary, we apply the latest observational data: the Union SNe Ia data, the nine observational Hubble data, the five-year WMAP and the SDSS baryon acoustic peak to constrain the GCG model as the unification of dark matter and dark energy. It can be seen that the evolution of EOS of dark energy for GCG is similar to quiescence, and the cosmological constant model is in 1σ confidence contour of the best fit dynamical $w_{de}(z)$. Furthermore, using the combined constraint to GCG model, it is shown that the best fit value of current EOS of DE $w_{0de} = -0.963 > -1$, and the confidence level is $w_{0de} = -0.963^{+0.047}_{-0.047} (1\sigma) \text{ } ^{+0.093}_{-0.094} (2\sigma)$. The values of transition redshift and current deceleration parameter are $z_T = 0.741^{+0.048}_{-0.050} (1\sigma) \text{ } ^{+0.096}_{-0.103} (2\sigma)$, $q_0 = -0.552^{+0.056}_{-0.055} (1\sigma) \text{ } ^{+0.112}_{-0.111} (2\sigma)$.

On the basis of the cosmic observations, we apply two diagnostics to distinguish GCG model and Λ CDM model. Since the evolution of $Om(z)$ for GCG model as the unification of dark matter and dark energy is not sensitive to density parameter Ω_{ob} , we use the Union SNe Ia data, the nine observational Hubble data, and a combined constraint to plot the evolution of $Om(z)$, respectively. It can be seen that, for the case of the Union SNe Ia data the difference between GCG model and Λ CDM model is obvious, while for the combined constraint and the OHD constraint, the best fit evolutions of $Om(z)$ for them are similar and the differences for these two models are not clear at 1σ and 2σ confidence level. Furthermore, on the basis of combined constraint, we get the best fit values and confidence levels of model parameters $A_s = 0.731^{+0.053}_{-0.059} (1\sigma) \text{ } ^{+0.090}_{-0.097} (2\sigma)$, $\alpha = -0.077^{+0.155}_{-0.126} (1\sigma) \text{ } ^{+0.277}_{-0.196} (2\sigma)$. This constraint on parameter α is more stringent than the results from Refs. [37][38]. Using the values of model parameters (A_s, α) obtained from Fig. 4 (a), we apply the statefinder parameters to discriminate the GCG and Λ CDM model. From r-s plane, it can be found that the difference for these two model is obvious.

Acknowledgments The research work is supported by NSF (10573003), NSF (10573004), NSF (10703001), NSF (10747113), NSF (10647110), and DUT (893326) of PR China.

-
- [1] A.G. Riess *et al*, 1998 *Astron. J.* **116** 1009 [arXiv:astro-ph/9805201]
[2] D.N. Spergel *et al*, 2003 *Astrophys. J. Suppl.* **148** 175 [arXiv:astro-ph/0302209]
[3] A.C. Pope *et al*, 2004 *Astrophys. J.* **607** 655 [arXiv:astro-ph/0401249]
[4] S. Weinberg, 1989 *Mod. Phys. Rev.* **61** 527
[5] B. Ratra and P.J.E. Peebels, 1988 *Phys. Rev. D.* **37** 3406
[6] R.R. Caldwell, M. Kamionkowski and N. N. Weinberg, 2003 *Phys. Rev. Lett.* **91** 071301 [arXiv:astro-ph/0302506]
M.R. Setare, 2007 *Eur. Phys. J. C* **50** 991
[7] B. Feng, X.L. Wang and X.M. Zhang, 2005 *Phys. Lett. B* **607** 35 [arXiv:astro-ph/0404224]
[8] A.Y. Kamenshchik, U. Moschella and V. Pasquier, 2001 *Phys. Lett. B* **511** 265 [arXiv:gr-qc/0103004]
P.X. Wu and H.W. Yu, 2007 *J. Cosmol. Astropart. Phys.* **0703** 015
[9] H.B. Benaoum, [arXiv:hep-th/0205140]
J.B. Lu, L.X. Xu, J.C. Li and H.Y. Liu, 2008 *Mod. Phys. Lett. A* **23** 25
S. Li, Y.G. Ma and Y. Chen, [arXiv:astro-ph/0809.0617]
[10] M. Li, 2004 *Phys. Lett. B* **603** 1 [arXiv:hep-th/0403127]
Q. Wu, Y.G. Gong, A.Z. Wang and J.S. Alcanizd, 2008 *Phys. Lett. B* **659** 34
[11] R.G. Cai, 2007 *Phys. Lett. B* **657** 228 [arXiv:hep-th/0707.4049]
[12] Using mathematical fundament, one expands equation of state of DE w_{de} or deceleration parameter q with respect to scale factor a or redshit z . For example, $w_{de}(z) = w_0 = \text{const}$ [13], $w_{de}(z) = w_0 + w_1 z$ [14], $w_{de}(z) = w_0 + w_1 \ln(1 + z)$ [15], $w_{de}(z) = w_0 + \frac{w_1 z}{1+z}$ [16], $q(z) = q_0 + q_1 z$ [13], $q(z) = q_0 + \frac{q_1 z}{1+z}$ [17], where w_0, w_1 , or q_0, q_1 are model parameters.
[13] A.G. Riess *et al*, 2004 *Astrophys. J.* **607** 665 [arXiv:astro-ph/0402512]

- [14] A.R. Cooray and D. Huterer, 1999 *Astrophys. J.* **513** L95 [arXiv:astro-ph/9901097]
- [15] B.F. Gerke and G. Efstathiou, 2002 *Mon. Not. R. Astron. Soc.* **335** 33 [arXiv:astro-ph/0201336]
- [16] E.V. Linder, 2003 *Phys. Rev. Lett.* **90** 091301 [arXiv:astro-ph/0208512]
- S. Nesseris and L. Perivolaropoulos, 2007 *J. Cosmol. Astropart. Phys.* **0702** 025 [arXiv:astro-ph/0612653]
- [17] L.X. Xu and J.B. Lu, accepted by *Mod. Phys. Lett. A*
- [18] B. Boisseau, G. Esposito-Farese, D. Polarski and A. A. Starobinsky, 2000 *Phys. Rev. Lett.* **85** 2236 [arXiv:gr-qc/0001066]
- [19] V. Sahni, Yu. Shtanov and A. Viznyuk, 2005 *J. Cosmol. Astropart. Phys.* **0512** 005 [arXiv:astro-ph/0505004]
- V. Sahni and Yu. Shtanov, 2003 *J. Cosmol. Astropart. Phys.* **0311** 014 [arXiv:astro-ph/0202346]
- [20] A.R. Liddle, 2004 *Mon. Not. R. Astron. Soc.* **351** L49 [arXiv:astro-ph/0401198]
- W. Godlowski and M. Szydlowski, 2005 *Phys. Lett. B* **623** 10 [arXiv:astro-ph/0507322]
- M. Biesiada, 2007 *J. Cosmol. Astropart. Phys.* **0702** 003 [arXiv:astro-ph/0701721]
- J.B. Lu, L.X. Xu, M.L. Liu and Y.X. Gui, 2008 *Eur. Phys. J. C* **58** 311C324
- J.B. Lu *et al*, 2008 *Phys. Lett. B* **662**, 87
- M. Szydlowski and W. Godlowski, 2006 *Phys. Lett. B* **633** 427 [arXiv:astro-ph/0509415]
- M. Szydlowski, A. Kurek and A. Krawiec, 2006 *Phys. Lett. B* **642** 171 [arXiv:astro-ph/0604327]
- [21] V. Sahni and T.D. Saini, A. A. Starobinsky and U. Alam, 2003 *JETP Lett.* **77** 201-206
- [22] V. Sahni, A. Shafieloo and A. A. Starobinsky, 2008 *Phys. Rev. D* **78** 103502 [arXiv:astro-ph/0807.3548]
- [23] U. Alam, V. Sahni, T. D. Saini and A. A. Starobinsky [arXiv:astro-ph/0303009]
- B.R. Chang *et al*, 2007 *J. Cosmol. Astropart. Phys.* **0701** 016 [arXiv:astro-ph/0612616]
- [24] E. Komatsu *et al*, [arXiv:astro-ph/0803.0547]
- [25] D. Rubin *et al*, [arXiv:astro-ph/0807.1108]
- [26] J. Simon *et al*, 2005 *Phys. Rev. D* **71**, 123001
- [27] J. Dunkley *et al*, [arXiv:astro-ph/0803.0586]
- [28] D.J. Eisenstein *et al*, 2005 *Astrophys. J.* **633**, 560 [arXiv:astro-ph/0501171]
- [29] P. Astier *et al*, 2006 *Astron. Astrophys.* **447** 31 [arXiv:astro-ph/0510447]
- [30] W.M. Wood-Vasey *et al*, [arXiv:astro-ph/0701041]
- [31] A.G. Riess *et al*, [arXiv:astro-ph/0611572]
- [32] M. Hamuy, M.M. Phillips, N.B. Suntzeff, R.A. Schommer and J. Maza, 1996 *Astron. J.* **112** 2408 [arXiv:astro-ph/9609064]
- S. Jha, A. G. Riess and R. P. Kirshner, 2007 *Astrophys. J.* **659** 122 [arXiv:astro-ph/0612666]
- [33] R.G. Abraham *et al*, 2003 *Astron. J.* **593** 622
- [34] T. Treu *et al*, 1999 *Mon. Not. R. Astron. Soc.* **308** 1037
- T. Treu *et al*, 2001 *Mon. Not. R. Astron. Soc.* **326** 221
- [35] J.R. Bond, G. Efstathiou and M. Tegmark, 1997 *Mon. Not. R. Astron. Soc.* **291**, L33 [arXiv:astro-ph/9702100]
- R. Lazkoz, E. Majerotto, 2007 *J. Cosmol. Astropart. Phys.* **0707** 015 [arXiv:astro-ph/0704.2606]
- [36] M. Makler, S.Q. Oliveira and I. Waga, 2003 *Phys. Rev. D* **68** 123521
- J.A.S. Lima, J.V. Cunha and J.S. Alcaniz, [arXiv:astro-ph/0611007]
- [37] Z.H. Zhu, 2004 *Astron. Astrophys.* **423** 421
- [38] P. Wu and H.W. Yu 2007 *Phys. Lett. B* **644** 16
- [39] D.J. Eisenstein and W. Hu, 1998 *Astrophys. J.* **496** 605 [arXiv:astro-ph/9709112]
- [40] U. Alam and V. Sahni, 2006 *Phys. Rev. D* **73** 084024 [arXiv:astro-ph/0511473]
- [41] S. Nesseris and L. Perivolaropoulos, 2007 *J. Cosmol. Astropart. Phys.* **0701**, 018 [arXiv:astro-ph/0610092]
- [42] W.L. Freedman *et al*, 2001 *Astrophys. J.* **553**, 47 [arXiv:astro-ph/0012376]
- [43] D. Kirkman *et al*, 2003 *Astrophys. J. Suppl.* **149** 1 [arXiv:astro-ph/0302006]
- [44] C.B. Netterfield *et al*, 2002 *Astrophys. J.* **571** 604 [arXiv:astro-ph/0104460]
- [45] C. Pryke *et al*, 2002 *Astrophys. J.* **568** 46 [arXiv:astro-ph/0104490]
- [46] S.W. Allen *et al*, 2004 *Mon. Not. R. Astron. Soc.* **353** 457, [arXiv:astro-ph/0405340]
- [47] M. Goliath *et al*, 2001 *Astron. Astrophys.* **380** 6 [arXiv:astro-ph/0104009]
- [48] J. V. Cunha, [arXiv:astro-ph/0811.2379]
- [49] T. Nakamura and T. Chiba, 1999 *Mon. Not. R. Astron. Soc.* **306** 696 [arXiv:astro-ph/9810447]
- [50] T.D. Saini, S. Raychaudhury, V. Sahni and A.A. Starobinsky, 2000 *Phys. Rev. Lett.* **85** 1162 [arXiv:astro-ph/9910231]
- [51] S. Nesseris and L. Perivolaropoulos, 2004 *Phys. Rev. D* **70** 043531
- U. Alam, V. Sahni, T.D. Saini and A.A. Starobinsky, 2004 *Mon. Not. R. Astron. Soc.* **354** 275
- [52] C.J. Feng, [arXiv:astro-ph/0809.2502]
- [53] E. M. Barboza Jr. and J. S. Alcaniz, 2008 *Phys. Lett. B* **666** 415-419 [arXiv:astro-ph/0805.1713]
- [54] U. Alam, V. Sahni, T.D. Saini and A.A. Starobinsky, 2003 *Mon. Not. R. Astron. Soc.* **344** 1057 [arXiv:astro-ph/0303009]
- [55] A. Shafieloo, U. Alam, V. Sahni and A. A. Starobinsky, 2006 *Mon. Not. R. Astron. Soc.* **366** 1081 [arXiv:astro-ph/0505329]